Pressure Sensitive Adhesion of an Elastomeric Protein Complex Extracted From Squid Ring Teeth

*Abdon Pena-Francesch, Bulent Akgun, Ali Miserez, Wenpeng Zhu, Huajian Gao, and Melik C. Demirel**

The pressure sensitive adhesion characteristic of a protein complex extracted from squid ring teeth (SRT), which exhibits an unusual and reversible transition from a solid to a melt, is studied. The native SRT is an elastomeric protein complex that has standard amino acids, and it does not function as adhesives in nature. The SRT can be thermally shaped into any 3D geometry (e.g., thin films, ribbons, colloids), and it has a glass transition temperature of 32 °C in water. Underwater adhesion strength of the protein film is approximately 1.5–2.5 MPa. The thermoplastic protein film could potentially be used in an array of fields, including dental resins, bandages for wound healing, and surgical sutures in the body.

1. Introduction

Pressure-sensitive adhesive (PSA) can adhere to a variety of surfaces with pressure contact, and can be classified according to their physical state (e.g., aqueous, solvent and hot melt).[1] The chemistry of the adhesive formulation is based on the polymer type, molecular weight, level of cross-linking, and additives (e.g., tackifiers, fillers, stabilizers, and plasticizers). Commercial PSA's are generally obtained from petroleum based chemicals, such as acrylics, acetates, nitriles, and special (e.g., styrene based) block copolymers. Although natural elastomers are used as adhesives (e.g., natural rubber,[2] soy bean protein[3]), to our knowledge, the number of reports related to bio-based PSA's is very limited. Additionally, natural PSA's typically have weak shear strength, and synthetic PSA's have cytotoxicity for medical uses.

There are other natural elastomers made from protein extracts, which have received significant interest as eco-friendly functional materials for underwater adhesion. Natural adhesives, such as mussel, sandcastle worm glue and gecko feet, provide adhesion in wet or dry conditions. Mussel adhesion[4] is based on a mixture of DOPA-containing proteins, which are able to provide various chemical-based surface interactions under wet conditions, including metal coordination,[5] hydrogen bonding,[6] and hydrophobic interactions.[7] Gecko feet rely on Van der Waals interactions by exploiting the principles of friction and wetting at nanoscale for dry[8] and wet[9] adhesion respectively. However, the adhesion of these natural elastomers is different from the pressure sensitive adhesion mechanism.

Here, we studied the pressure-sensitive adhesive characteristics of a natural protein complex extracted from European common squid (*Loligo vulgaris*). Squid ring teeth (SRT) is a thermoplastic hot melt PSA, which is plasticized by water above its glass transition temperature (T_g = 32 °C). SRT does not require any drying process or toxic solvents, and have good adhesion strength to a range of substrates at low temperatures. Due to its high tensile (≈1.5 MPa) and shear strength (≈2.5 MPa) in wet conditions and its natural biocompatibility, SRT provides unique opportunities of utilization as a hot melt adhesive.

An invertebrate in the cephalopod class of the phylum Mollusca that uses its limbs and suckers for a variety of tasks including holding prey, locomotion, and behavioral displays[10] in cold sea water (i.e., 5–15 °C), squids have evolved teeth inside their suckers, which serve to swiftly grasp preys underwater.[11] Typically, the muscles on the squid limbs generate large pressure differences at the suckers for holding a wide variety of objects.[12] Although SRT is strictly made of proteins which are stabilized by hydrogen bonding and hydrophobic

A. Pena-Francesch, Prof. M. C. Demirel
Materials Research Institute
and Department of Engineering Science and Mechanics
Pennsylvania State University
University Park
PA 16802, USA
E-mail: mdemirel@engr.psu.edu
Dr. B. Akgun
Center for Neutron Research
National Institute of Standards and Technology
Gaithersburg, MD 20899, USA
Dr. B. Akgun
Department of Materials Science and Engineering
University of Maryland
College Park, MD 20742, USA
Dr. B. Akgun
Department of Chemistry
Boğaziçi University
Bebek, Istanbul 34342, Turkey
Dr. A. Miserez
School of Materials Science and Engineering and
School of Biological Sciences
Nanyang Technological University
50 Nanyang Avenue
639798, Singapore
Dr. W. Zhu, Prof. H. Gao
Division of Engineering
Brown University
Providence, RI 02912, USA

DOI: 10.1002/adfm.201401534

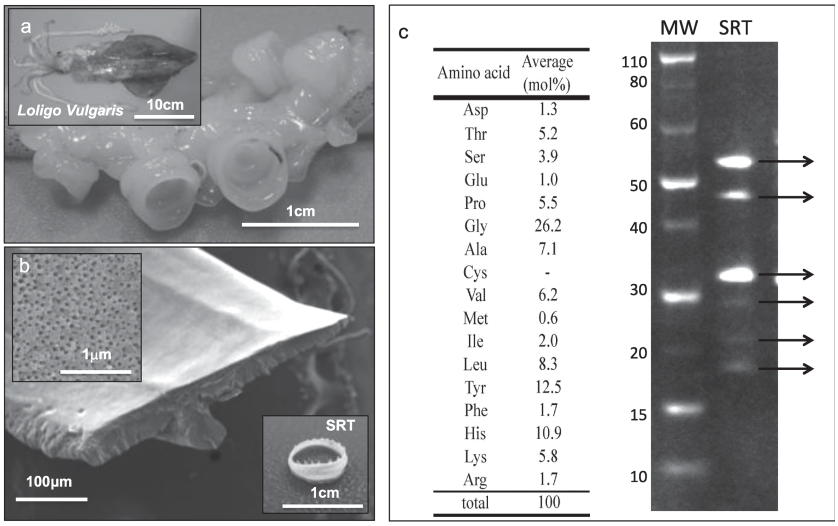

Amino acid	Average (mol%)
Asp	1.3
Thr	5.2
Ser	3.9
Glu	1.0
Pro	5.5
Gly	26.2
Ala	7.1
Cys	-
Val	6.2
Met	0.6
Ile	2.0
Leu	8.3
Tyr	12.5
Phe	1.7
His	10.9
Lys	5.8
Arg	1.7
total	100

Figure 1. European common squid (*Loligo vulgaris*) a) captured in Catalan waters (inset), shows a close-up picture of the suckers located in the tentacles, which contain the proteinaceous SRTs. b) Cross-sectional SEM and optical image reveal a highly organized structure of nanopores and a ring structure respectively. c) SDS-Page and amino acid composition of SRT.

interactions,[13] it is mainly functional in cold seawater with no known functions at elevated temperatures (e.g., >32 °C) based on its attachment biomechanics.

2. Results

SRT were extracted from European squid suckers, which are located along the muscular arms and tentacles (**Figure 1**a). Optical and electron microscope images show that SRT has a ring structure with nanoscale pores (Figure 1b). The internal structure of the SRT consists of an array of aligned nanopores with an average diameter of 160 ± 33 nm. The amino acid composition and the protein gel electrophoresis results of SRT are shown in Figure 1c. The amino acid composition shows high composition of glycine and histidine accounting for approximately 40–50% of total amino acids. The chain flexibility, in the melt phase, required for rubberlike elasticity is likely achieved in SRT protein through the use of glycine.[14] The high content of histidine is also an important feature in load bearing and impact resistance tissues because of the versatility of the imidazole side-chain to stabilize protein networks, for instance through hydrogen-bonding, metal coordination complexation[5] or covalent cross-linking.[15] In **Table 1**, the amino acid composition of SRT is also compared with commonly observed noncrystalline bioelastomers[16] (e.g., elastin,[17] resilin,[18] and abductin[19]). Compared with these bioelastomers, the proteinaceous structure of the SRT does not have any covalent cross-linker and, hence, dissolves in weak alkaline or acidic buffers. High nonpolar to polar ratio of the amino acid side groups of SRT and other bioelastomers listed in Table 1 suggest that the chains would be well separated by the presence of solvent molecules (where resilin is an exception for the polarity ratio and the mechanism is described elsewhere[18]. Additionally, the high content of tyrosine residues (10–15%) suggests the ability to form hydrogen bonds with -OH groups of Tyr in the swelled state.[20] Consequently, the native SRT swells 15% to 20% by volume when immersed in water. Swelling of the protein film also increases with temperature (i.e., 20% ± 3 at 45 °C and 35% ± 3 at 75 °C respectively by volume with reference to 30 °C).

Table 1. Summarized compositional information.

Side chain	Occurrence in proteins[21]	SRT[a)]	SRT[b)]	Elastin[c)]	Abductin[c)]	Resilin[c)]
Small[d)]	21.1	39.5	47.4	54.9	70.2	62.0
Nonpolar	39.9	38.4	37.4	60.9	28.5	22.0
Polar	22.1	9.1	7.2	7.5	13.1	35.0

[a)] *Loligo vulgaris*; [b)] *Dosidicus gigas*;[13] [c)] Adapted from Erman et al.;[22] [d)] Small aminoacids are Gly, Val, Ala.

The isoelectric point of the protein film (**Figure 2**a) is measured using zeta-potentiometer. The net charge on the protein film is close to zero at physiological buffers (e.g., pH ≈ 7), which is to be expected since the major charged residue in SRTs is histidine whose pKa is 6.5. The net charge of the dry protein complex is also measured by a Kelvin probe, and its magnitude ranges from 0.2 to 0.4 nC/cm^2 depending on the relative humidity of the sample. The glass transition is analyzed using the differential scanning calorimetry (DSC). The glass transition temperature is 32 °C in water (Figure 2b), showing a transition peak for the heat capacity (inset). The SRT can be thermally processed to form a melt and shaped into any 3D geometry, such as films, ribbons, tubes or thin films. For example, Figure 2c shows the protein film prepared by thermal processing, and Figure 2d demonstrates the effect of surface tension on the smoothing of a colloid from irregular SRT powder. The thermoplastic effect of temperature on the SRT protein complex is similar to a polymer melt.[23]

The protein melt shows a peculiar underwater adhesive response, although the native (i.e., prior to processing) SRT is not adhesive in water or dry conditions. It is not adhesive below its glass transition temperature, but only adhesive when processed above its glass transition temperature. Pictures of single-lap joints bonded with SRT protein are shown in **Figure 3**a,b for wet and dry testing condition respectively. Analysis of the unbounded surfaces show that the failure is adhesive (i.e., failure at the substrate-protein interface) for the wet case, but cohesive for the dry case.

The adhesion strength increases abruptly (i.e., two orders of magnitude) above a critical preload pressure, as shown in **Figure 4**a. The temperature for secure bonding at 45 °C or 70 °C provide similar adhesion strength but higher preload is required for the former. The adhesive is stable underwater at least for six months. The normal tensile adhesion strength of the protein film is approximately 1.50 ± 0.23 MPa for underwater and 0.24 ± 0.08 MPa for dry conditions. The lack of any

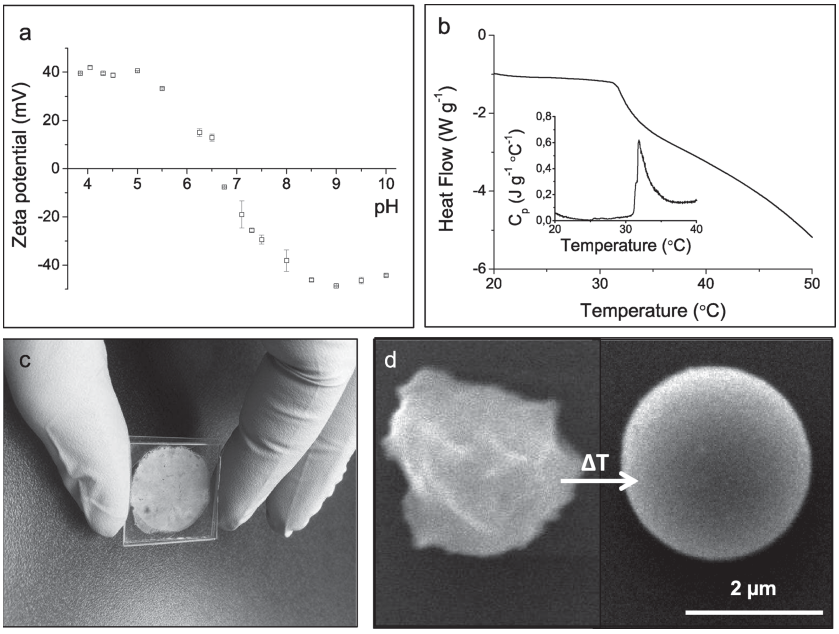

Figure 2. a) The isoelectric point (pH = 6.7) and zeta potential as a function of pH for the protein-melt extracted from the European SRT. b) DSC of the protein melt for the heat flow and C_p (inset) of protein melt in water show a glass transition at 32 °C. c) Optical image of SRT protein complex bonded in between two-glass substrates. d) Smoothing of SRT powder driven by the tendency to reduce surface energy.

chemical cross-linker (including cysteine residues) in SRT amino acid composition shows that the covalent bonding could not explain the adhesion mechanism of SRT alone, as discussed in the next section. Figure 4b shows adhesion strength of the protein film as a function of temperature in dry and underwater conditions. The dry experiment is performed after keeping the samples overnight in a vacuum desiccator. Figure 4c shows the adhesion data for various surfaces including glass, hydrophilic polymeric surfaces (polylactide, PLA, and polyvinyl acetate, PVA), and plasma-treated (i.e., to create hydroxyl sites on the polymer surface for improved adhesion) hydrophobic surfaces (polystyrene, PS, and Polydimethylsiloxane, PDMS). The protein film only adheres to hydrophilic surfaces but doesn't adhere to hydrophobic surfaces underwater. Therefore, we oxidized the surface of these polymers with corona treater. We also measured the normal tensile adhesion strength for the SRT protein film extracted from *Dosidicus gigas* (Humboldt squid)[13] for underwater and dry conditions (i.e., 1.12 ± 0.08 MPa and 0.63 ± 0.16 respectively). These values are similar to the adhesion strength of the protein film extracted from *Loligo vulgaris*. We should note that tensile tests provide qualitative comparison between various substrates (i.e., glass and polymer bonding) as well as experimental conditions (i.e., temperature, pH and ion concentration). The adhesion strength of SRT protein complex were quantitatively measured by shear tests according to the ASTM standard 3163. Single-lap underwater shear adhesion strength (i.e., 2.51 ± 0.55 MPa for underwater and 0.17 ± 0.05 MPa for dry conditions) is larger than that in tension (Figure 4d), which is common for soft materials.[24] We have also performed experiments to test the effects of pH and salt additions (**Figure 5**), which show that the addition of salt substantially reduces the adhesion strength (Figure 5a) but pH has no effect on the adhesion strength in mild conditions (Figure 5b). Strong acid or base conditions dissolve the SRT film, and hence a cohesive failure is observed (Figure 5b).

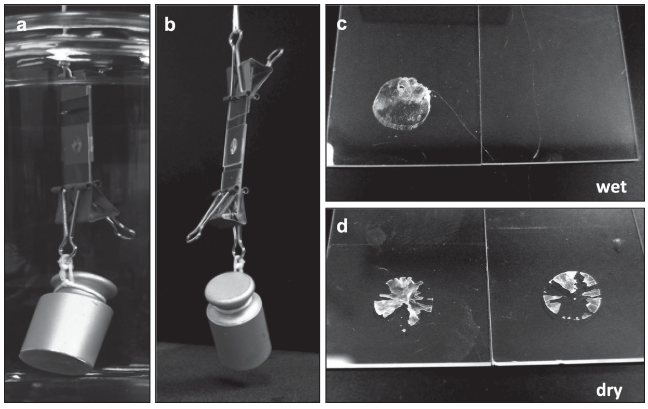

Figure 3. Pictures of lap joints bonded with SRT protein complex in a) wet and b) dry testing conditions. Glass substrates were holding a 300 g weight for both cases. Tested and separated substrate surfaces show c) adhesive and d) cohesive failure mechanisms for wet and dry conditions.

We investigated the molecular morphology of the protein film using small angle neutron scattering (SANS) at three temperatures (i.e., 20°, 45°, and 70 °C) in the following order: wet (**Figure 6**a), dry (Figure 6b), and rewetted (Figure 6c) conditions. The data reveals (**Table 2**) a structure peak for wet conditions at in-plane wave-vector, q, value of approximately 0.007 Å^{-1} (i.e., indicating that there is a large globular structure), which corresponds to domain-domain distance of ≈ 90 nm. The deuterated water filling these domains enhances the neutron contrast between the pores and the matrix, which gives stronger scattering signal. The peak at the SANS spectra is independent of the temperature variations, and peak intensities are stronger for the wet and rewetted conditions than the dry condition. The peak becomes weaker and broader when the sample is dried at 70 °C overnight. The radius of gyration of domains for wet and dry cases are calculated from smeared Beaucage model[25] consecutively and reported in Table 2. SANS data for wet and rewet cases also shows the reversibility of the process. The same structure is obtained after drying and rehydrating the protein film. We have also conducted neutron experiments under preload (Figure 6d) of 2.6 MPa. It is clear from the neutron data that there is no structural change between unloaded and preloaded samples.

3. Discussion

The adhesion experiments could be divided into two categories (i.e., above and below glass transition temperature, T_g). First,

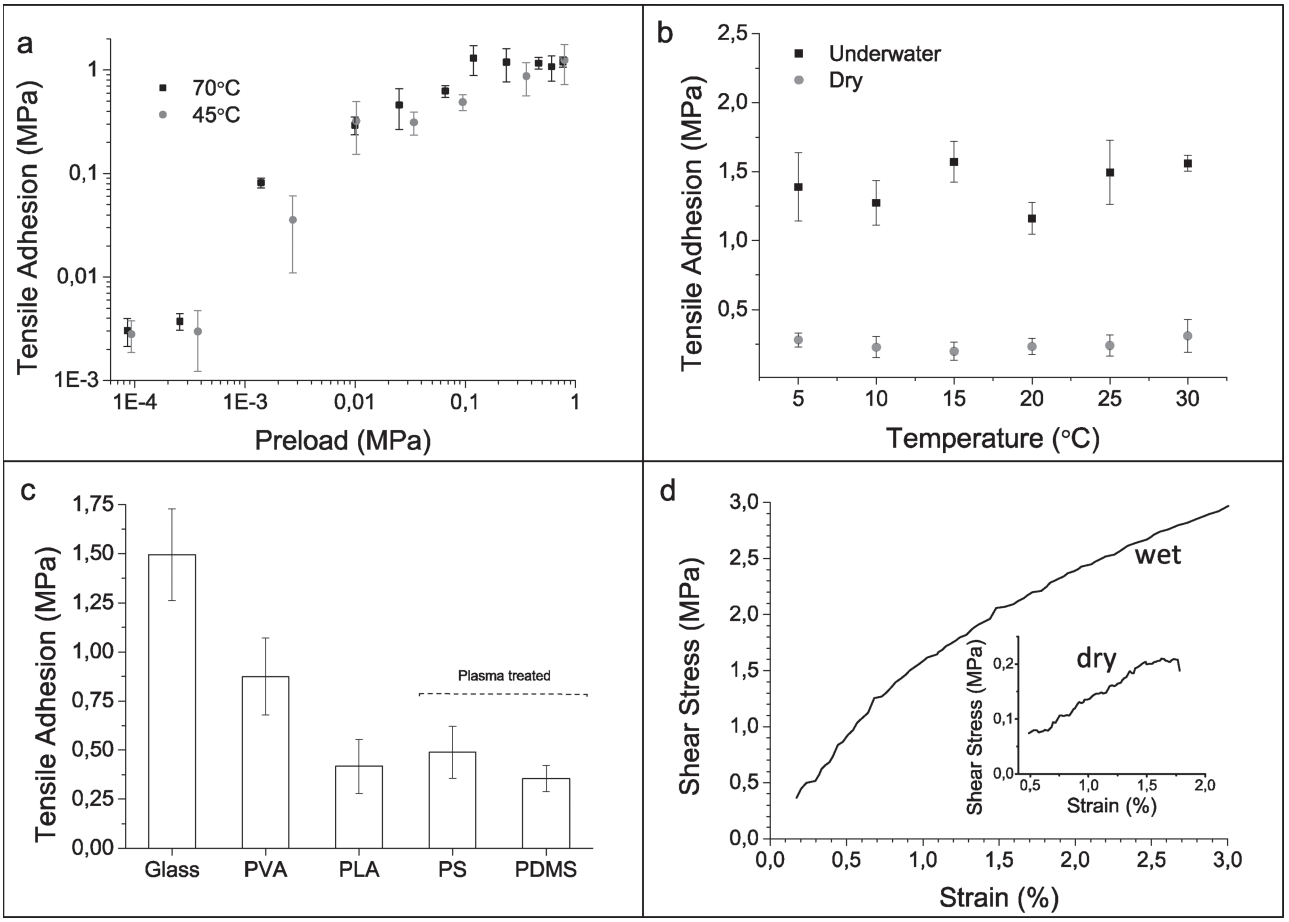

Figure 4. a) Normal tensile adhesion strength of SRT protein complex at room temperature as a function of the preload at 45 °C and 70 °C melt temperature. b) The adhesion strength is measured underwater and dry conditions between 5 to 30 °C. c) Underwater adhesion strength for various surfaces: glass, hydrophilic polymeric surfaces (PLA and PVA), and plasma treated hydrophobic polymeric surfaces (PS, PDMS) at room temperature. d) Single-lap shear adhesion strength in wet and dry conditions. Poly(vinyl acetate) (PVA, MW 1 500 000, Polysciences, Inc.) and polylactide (PLA, polylactide resin, NatureWorks) polymer substrates were prepared by dissolving PVA in methanol and PLA in dichloromethane and spin-coating on glass substrates with an approximate thickness of 500 µm.

for the case below T_g, the protein film is not adhesive because it is very stiff (i.e., modulus of ≈1 GPa)[26] and the deformation is limited under compressive loading. Second, for the case above T_g, the material is soft (i.e., ≈ 10 MPa) and deforms easily, which increases the total area of contact with the surface. Therefore, the adhesion increases via nonspecific Van der Waals interactions. When cooled below T_g, the material modulus increases by two orders of magnitude (i.e., ≈1 GPa), and the adhesion strength increases drastically because of lowered roughness and shielded charge in water (i.e., the dielectric constant of air is one, however in water it is 80). The domains observed in SANS studies provide compliant adhesion control (similar to crack trapping)[27] at the nanoscale in the wet condition. These domains help water to escape when the film is pressed and shield the charge.

The mechanism of adhesion could be due to several effects combining chemistry, surface roughness, residual stresses at the interface or mechanical instability. We proposed a "heuristic" coarse-grained computational model, which makes the assumption that the effect of the preload is an elastic instability combined with a tri-block charge distribution. The details of the model are discussed in the Supplementary Information. The tri-block model is used to mimic the nanoscale domain formation without the detailed protein sequence of the structure. Although our approach presents a local contact model that explains the difference between wet and dry adhesion, the adhesion strength predicted by the model is quantitatively much higher than the experimental values. Compared to the tri-block model, it is certainly worth considering other possibilities. It is well known that microscale roughness greatly affects adhesion strength and makes it respond to preload.[28] However, it cannot explain the difference between dry and wet adhesion. In fact, a model based on microscale roughness would predict that the preload effect should be higher under dry conditions than under wet conditions, which obviously contradicts our experiments. Indeed, due to high moduli, we would expect defective contact at the interface and a substantial preload would be expected to establish full molecular contact. Alternatively, the nature of the interface contact could change the properties of the adhesive in a complex way (e.g., water content changes simultaneously with temperature creating important stresses at the interface). Therefore, residual stresses formed during the melting could

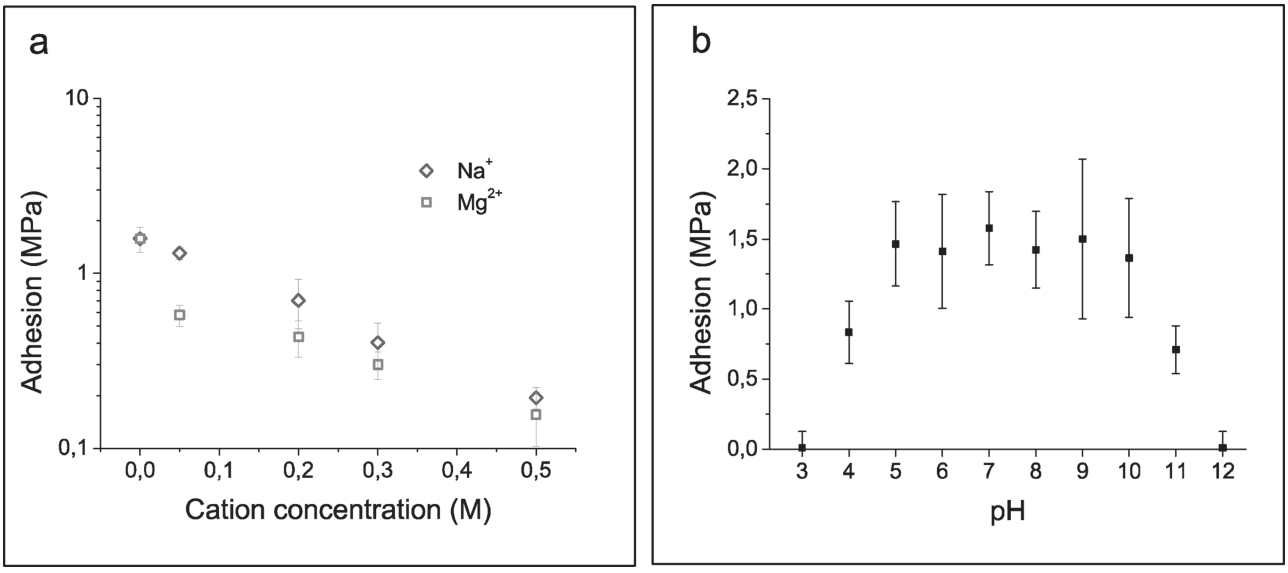

Figure 5. Normal tensile adhesion strength as a function of a) salt concentration, and b) pH are shown.

be a potential mechanism too. However, this model cannot explain why there exists such a difference between dry and wet adhesion strengths, with the latter much higher than former, contrary to the conventional understanding of adhesion. In summary, there is no complete model to explain the complexities of the new phenomenon observed for the adhesion of the SRT protein complex, and further studies are needed to explain the adhesion mechanism.

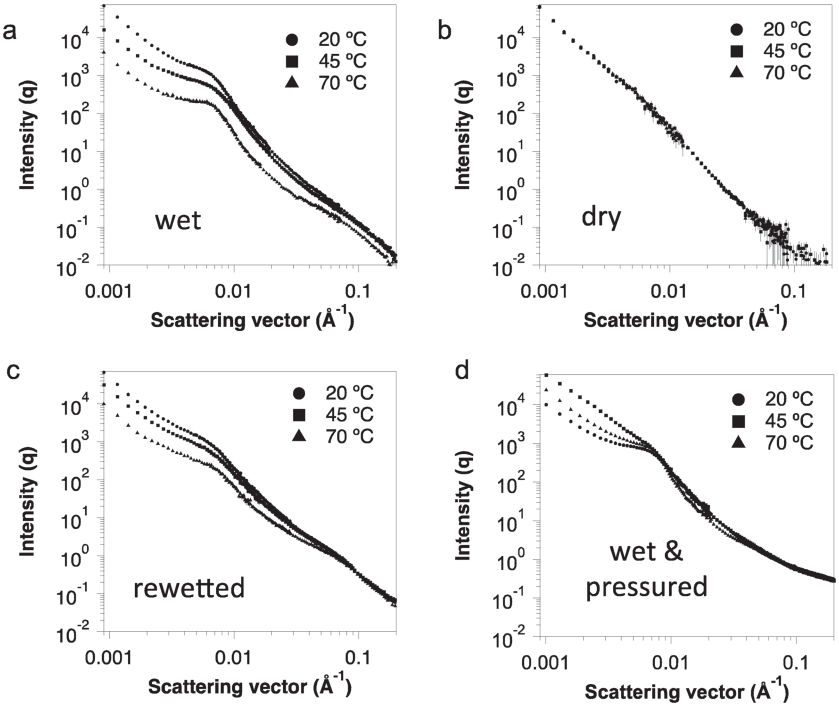

Figure 6. Nanoscale domain characterization via neutron scattering. a) SANS data of the protein-melt shows the existence of a large domain at three temperatures in wet conditions. The small domain b) disappears when the protein film dried, but it c) reappears if the film is rewetted. d) The experiment is repeated under preload of 2.6 MPa and wet conditions.

4. Conclusion

We studied the adhesion characteristic of a protein complex extracted from squid ring teeth. SRT protein complex exhibit an unusual and reversible transition from solid to melt, and hence it can be molded. The native SRT is an elastomeric protein complex that has standard amino acids, and does not function as adhesives in nature. Therefore, the adhesion mechanism of SRT is surprising. The structure-function relationship of SRT will be the focus of our future studies, which could lead to a novel biodegradable type of load-bearing thermoplastic. The bioelastomer adhesive could be used in an array of fields in the future, including dental resins, bandages for wound healing, and surgical sutures in the body, all of which require wet adhesion.

5. Experimental Section

SRT Collection: European common squids (*Loligo vulgaris*) are caught from the coast of Tarragona (Spain). The squid ring teeth (SRT) are removed from the tentacles and immediately soaked in deionized (DI) water and ethanol mixture (70:30 ratio v/v) overnight. After vacuum drying, the rings are pulverized in liquid nitrogen using a ceramic mortar and pestle.

Table 2. SANS results of the SRT protein complex.

Temperature	Radius of Gyration R_g [nm]		
	Wet	Dry	Rewetted
20 °C	56.7 ± 0.1	102.3 ± 17.9	67.2 ± 4.7
45 °C	51.4 ± 0.3	105.3 ± 9.3	63.2 ± 5.2
70 °C	52.5 ± 0.2	106.7 ± 9.7	61.7 ± 6.8

SRT Melting: 25 mg of SRT powder is mixed with 10 mL of deionized water above its glass transition temperature (e.g., 45 °C or 70 °C). The powder can be melted at temperatures lower than 70 °C, but it may take a longer time (i.e., > 1 minute) to complete the thermal process. The elastomer is gently pressed to melt into a flat thin film with an area of 1 cm^2, and then cooled at room temperature for testing. The thickness of the film is approximately 200 μm. The powder may disperse during the melting process due to electrostatic, surface tension and capillary forces. If the film is not uniform, the thermal process could be repeated multiple times.

Protein Analysis: SRT is dissolved in 10% acetic acid/2M urea solution, and subjected to sodium dodecyl sulfate polyacrylamide gel electrophoresis (SDS-PAGE) for protein separation. The protein gels were stained with Coomassie blue. For amino acid analysis, SRT were hydrolyzed in vacuum in 6M HCl/5% phenol overnight, washed on a vacuum evaporator with methanol (SpeedVac), and analyzed on a post-column derivatization (Ninydrin-based S433 Sykam analyzer). This technique for amino acid composition determination has been previously used in SRT proteins extracted from Humboldt Squid.[13]

Differential Scanning Calorimetry: The glass transition temperature, T_g, of the SRT protein complex is determined by a differential scanning calorimeter (Perkin Elmer DSC 8500). 10 mg of SRT with ultrapure MiliQ water (1:1 ratio w/w) were mixed and sealed in a 40 μL stainless steel pan. The temperature scanning range was 10 to 90 °C at a heating rate of 5 °C/min.

Charge Measurements: The ZetaSpin[29] measures the zeta potential of a disk-shaped sample rotated at 1000 rpm using a conductivity probe. The protein film is melted on a 1-inch (in diameter) glass sample above its glass transition temperature, pressed gently to spread the film uniformly, and then cooled to room temperature for testing. The pH probe is calibrated with standard solutions. The pH is varied by 0.5 units, and measured in the range of 3–11.

Adhesion Tests: Tensile and shear tests are performed to estimate the adhesion strength. At least 5 individual tests were performed to ensure statistical significance. Single lap shear adhesion (Figure 3d) was measured in a universal testing machine (United Calibration Corp., STM-20) at 1.27 mm/min strain rate (0.05 inch/min). Adhesive joints were prepared according to ASTM 3163 standard with glass substrates. The adhesive joints were kept underwater initially, and were dried overnight at room temperature for dry adhesion measurement. Single lap shear adhesion was validated using commercially available ethyl cyanoacrylate ("Superglue") and epoxy ("Loctite 5 minute epoxy") glues. These samples were cured for 24 h at room temperature. The adhesion strengths are 3.39 ± 0.60 MPa for ethyl cyanoacrylate and 4.75 ± 1.42 MPa for epoxy for dry conditions. Tensile adhesion strength normal to the substrate surface was determined in a home-built setup with a liquid media reservoir for both underwater and dry adhesion. The glass slides (plain VWR micro slides, 1 mm thick) were pulled apart in the normal direction of the substrate surface (opening mode). Normal tensile adhesion tests at different salt concentration and pH are immersed in the respective solutions. Ultrapure water is titrated with acetic acid and sodium hydroxide to prepare solutions between pH 3 and 12. NaCl and $MgCl_2$ salts are dissolved in ultrapure water between 0.05 M and 0.5 M (Na^+ and Mg^{2+}) for salt concentration experiments.

Small-Angle Neutron Scattering (SANS): Data is acquired on the NG-7 SANS beam-line at the National Institute of Standards and Technology (NIST) Center for Neutron Research (NCNR) in Gaithersburg, MD. Approximately 30 mg of pulverized SRT and 0.44 mg of D_2O are heated at 70 °C for 2 minutes to melt the protein. The protein melt is sandwiched between two quartz windows of 1-inch in diameter, and placed in adjustable standard titanium SANS cell. Scattering data is collected from an identical empty cell without the sample for background correction. The data is also corrected for detector sensitivity and electronic noise. Direct beam measurements are taken to convert the raw data intensities to an absolute scale. All the SANS data are reduced and analyzed using Igor Pro NCNR SANS software following the standard methods.[30] The SANS data is collected using wavelength, λ, of 8.09 Å and four different detector distances; 1 m, 4 m, 13 m, and 15.3 m with lenses to obtain a q range of 0.001 $Å^{-1}$ to 0.4 $Å^{-1}$ where $q = (4\pi/\lambda)\sin\theta$ where 2θ is the scattering angle. Two- and one-level smeared Beaucage model[25] is fitted for wet and dry samples respectively, and are reported in Table 2. Beaucage model[25] is an empirical model and it provides good estimates for the radius of gyration, R_g. SANS measurements under hydrostatic pressure were performed using a hydraulic pressure cell that permits in situ measurements over a pressure range from 1 to 300 MPa and over a T range spanning 25–190 °C.

Supporting Information

Supporting Information is available from the Wiley Online Library or from the author.

Acknowledgements

The authors thank Boualem Hammouda at NIST for helpful discussions on SANS data. The authors gratefully acknowledge financial support for this work from the Office of Naval Research (N000141310595) and the Pennsylvania State University. AM was supported from a Singapore Ministry of Education Tier 2 grant (MOE2011-T2–2–044). Certain commercial equipment, instruments, or materials are identified in this paper to foster understanding. Such identification does not imply recommendation or endorsement by the National Institute of Standards and Technology, nor does it imply that the materials or equipment identified are necessarily the best available for the purpose. M.C.D. planned, developed and supervised the research. M.C.D. and A.P.F. introduced the protein melt concept and its adhesive properties, characterized the surfaces, and performed the spectroscopic, mechanical and adhesion experiments. B.A. performed the SANS experiments. W.Z. and H.G. developed the computational model based on the comments received from M.C.D. A.M. performed biochemical analyses, and provided comments on SRT biochemistry. B.A. and A.M. provided editorial comments. M.C.D. and H.G. contributed to writing and revising the manuscript, and all authors agreed on its final contents.

Received: May 12, 2014
Revised: June 5, 2014
Published online: August 11, 2014

[1] I. Benedek, *Pressure-sensitive adhesives and applications*, CRC Press, New York **2004**.
[2] I. Khan, B. Poh, *J. Polym. Environ.* **2011**, *19*, 793.
[3] Z. Zhong, X. S. Sun, D. Wang, J. A. Ratto, *J. Polym. Environ.* **2003**, *11*, 137.
[4] P. L. Lee, P. B. Messersmith, J. N. Israelachvili, J. H. Waite, *Annu. Rev. Mater. Res.* **2011**, *41*, 99.
[5] J. Yu, W. Wei, M. S. Menyo, A. Masic, J. H. Waite, J. N. Israelachvili, *Biomacromolecules* **2013**, *14*, 1072.
[6] T. H. Anderson, J. Yu, A. Estrada, M. U. Hammer, J. H. Waite, J. N. Israelachvili, *Adv. Funct. Mater.* **2010**, *20*, 4196.

[7] W. Wei, J. Yu, C. C. Broomell, J. N. Israelachvili, J. H. Waite, *J. Am. Chem. Soc.* **2013**, *135*, 377.
[8] K. Autumn, M. Sitti, Y. A. Liang, A. M. Peattie, W. R. Hansen, S. Sponberg, T. W. Kenny, R. Fearing, J. N. Israelachvili, R. J. Full, *Proc. Natl. Acad. Sci. U.S.A.* **2002**, *99*, 12252.
[9] A. Y. Stark, I. Badge, N. A. Wucinich, T. W. Sullivan, P. H. Niewiarowski, A. Dhinojwala, *Proc. Natl. Acad. Sci. U.S.A.* **2013**, *110*, 6340.
[10] A. Packard, *Biol. Rev.* **1972**, *47*, 241.
[11] L. W. Williams, *The Anatomy of the Common Squid, Loligo Pealii: Lesueur*, Library and printing-office late EJ Brill, New York **1910**.
[12] A. Smith, *J. Exp. Biol.* **1996**, *199*, 949.
[13] A. Miserez, J. C. Weaver, P. B. Pedersen, T. Schneeberk, R. T. Hanlon, D. Kisailus, H. Birkedal, *Adv. Mater.* **2009**, *21*, 401.
[14] A. S. Tatham, P. R. Shewry, *Philos. Trans. R. Soc., B* **2002**, 357.
[15] C. C. Broomell, R. K. Khan, D. N. Moses, A. Miserez, M. G. Pontin, G. D. Stucky, F. W. Zok, J. H. Waite, *J. R. Soc., Interface* **2007**, *4*, 19.
[16] a) M. Gosline, *The Mechanical Properties of Biological Materials*, Company of Biologists Limited, UK **1980**; b) J. Gosline, M. Lillie, E. Carrington, P. Guerette, C. Ortlepp, K. Savage, *Philos. Trans. R. Soc., B* **2002**, *357*, 121.
[17] K. Dorrington, N. McCrum, *Biopolymers* **1977**, *16*, 1201.
[18] G. Qin, X. Hu, P. Cebe, D. L. Kaplan, *Nat. Commun.* **2012**, *3*, 1003.
[19] Q. Cao, Y. Wang, H. Bayley, *Curr. Biol.* **1997**, *7*, R677.
[20] C. N. Pace, G. Horn, E. J. Hebert, J. Bechert, K. Shaw, L. Urbanikova, J. M. Scholtz, J. Sevcik, *J. Mol. Biol.* **2001**, *312*, 393.
[21] G. Trinquier, Y.-H. Sanejouand, *Protein Eng.* **1998**, *11*, 153.
[22] B. Erman, J. E. Mark, *Structures and Properties of Rubberlike Networks*, Oxford University Press, USA **1997**.
[23] P. De Gennes, L. Leger, *Annu. Rev. Phys. Chem.* **1982**, *33*, 49.
[24] A. Parness, D. Soto, N. Esparza, N. Gravish, M. Wilkinson, K. Autumn, M. Cutkosky, *J. R. Soc., Interface* **2009**, *6*, 1223.
[25] G. Beaucage, *J. Appl. Crystallogr.* **1995**, *28*, 717.
[26] P. A. Guerette, S. Hoon, Y. Seow, M. Raida, A. Masic, F. Tian, M. C. Demirel, A. Pena-Francesch, S. Amini, G. Tay, A. Miserez, *Nat. Biotechnol.* **2013**, *31*, 908.
[27] N. J. Glassmaker, A. Jagota, C.-Y. Hui, W. L. Noderer, M. K. Chaudhury, *Proc. Natl. Acad. Sci. U.S.A.* **2007**, *104*, 10786.
[28] S. Kim, M. Sitti, *Appl. Phys. Lett.* **2006**, *89*, 261911.
[29] P. J. Sides, J. D. Hoggard, *Langmuir* **2004**, *20*, 11493.
[30] S. R. Kline, *J. Appl. Crystallogr.* **2006**, *39*, 895.